Geochemical Perspectives Letters

Crustal controls on light noble gas isotope variability along the Andean Volcanic Arc

J. Lages[1*], A.L. Rizzo[2], A. Aiuppa[1,2], P. Robidoux[3], R. Aguilar[4], F. Apaza[4], P. Masias[4]

doi: 10.7185/geochemlet.2134

Abstract

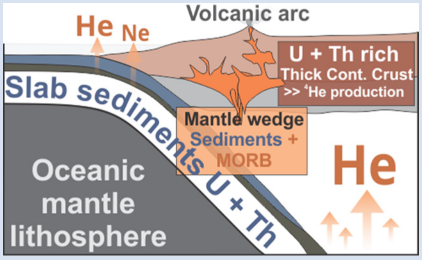

This study combines new noble gas data from fluid inclusions in minerals from Sabancaya, Ubinas, and El Misti (CVZ, Peru) and Villarica (South Chile, SVZ) with a revised noble gas compilation in the Andes, to identify systematic along arc variations in helium isotope compositions. We find $^3He/^4He$ ratios varying from 8.8 R_A (Colombia) to 7.4 R_A (Ecuador) within the NVZ, and only as high as 6.4 R_A in the CVZ (R_A is the atmospheric $^3He/^4He$ ratio of 1.39×10^{-6}). These distinct isotope compositions cannot be explained by variable radiogenic ^4He production *via* slab fluid transport of U and Th in the mantle wedge, since both NVZ and CVZ share similar slab sediment inputs (Th/La $\approx$ 0.08–0.13). Instead, the progressively more radiogenic $^3He/^4He$ signatures in Ecuador and Peru reflect ^4He addition upon magma ascent/storage in the crust, this being especially thick in Peru (>70 km) and Ecuador (>50 km) relative to Colombia (~30–45 km). The intermediate compositions in the North (8.0 R_A) and South (7.9 R_A) Chile, both high sediment flux margins, mostly reflect a more efficient delivery of radiogenic He in the wedge from the subducted (U-Th-rich) terrigenous sediments. Our results bring strong evidence for the major role played by crustal processes in governing noble gas compositions along continental arcs.

Received 19 May 2021 | Accepted 22 October 2021 | Published 23 November 2021

Introduction

Subduction zones are the main drivers of volatile exchange between the Earth's interior reservoirs and the atmosphere (Zellmer *et al.*, 2015). Studying the chemical and isotopic imprints of arc-related fluids is key to resolve their origin and fate along convergent margins (Hilton *et al.*, 2002). Noble gases in arc magmatic/hydrothermal fluids, and trapped as fluid inclusions (FIs) in minerals, are fundamental tracers of the relative contributions of potential sources at work in an arc context: the mantle, the subducted slab, and the arc crust (Sano and Fischer, 2013).

Poreda and Craig (1989) were among the first to investigate arc gas emissions for their noble gas isotope compositions. They reported $^3He/^4He$ ratios close to those found in MORBs (8 ± 1; Graham, 2002), implying a dominant helium origin from the mantle wedge above the subducted plate. However, Hilton *et al.* (2002) estimated an average of 5.4 R_A for volcanic arc gases globally. Lower than MORB $^3He/^4He$ ratios have been explained invoking either (i) assimilation of ^4He-rich crustal fluids during magma crustal storage/ascent (*e.g.*, Mason *et al.*, 2017), or (ii) addition of radiogenic ^4He to the mantle wedge (Hanan and Graham, 1996) *via* subducted slab sediments (if U + Th-rich sediments are involved; Kagoshima *et al.*, 2015).

The Andean volcanic arc offers a unique opportunity to evaluate the crust *versus* slab hypotheses. The ~7000 km long arc is subdivided into four volcanic zones (VZs), three of which are investigated here (Northern VZ, Colombia and Ecuador; Central VZ, Peru and North Chile; and Southern VZ, South Chile). Ancellin *et al.* (2017) and Mamani *et al.* (2010) noted, for the Ecuadorian and Peruvian arcs, respectively, high degrees of crustal assimilation by magmas erupted in the region. Along the trench, the age of the subducted oceanic floor (46.2 Ma in North-Central Chile to 10.3 Ma in South Chile; Syracuse *et al.*, 2010) and the degree of obliquity of the subducted slab (similar across the active volcanic zones) are other key factors impacting magma genesis and distribution of active volcanism in the Andes (Stern, 2004). Moreover, slab contributions have been noted in the C content of volcanic gas emissions (Aiuppa et al., 2017), whose compositions strongly correlate with the nature of subducted sediments in each region (Plank, 2014). However, in addition to the role of the slab, crustal processes have also been invoked (Hidalgo *et al.*, 2012), especially for noble gases compositions previously reported for the continental arc (*e.g.*, Hilton *et al.*, 1993).

Here, we present the very first noble gas data from Sabancaya, Ubinas, and El Misti (Central Volcanic Zone, Peru) and report on new noble gas chemical and isotope compositions for Villarica (South Chile). These were obtained from the analyses of bulk (primary and secondary) fluid inclusion compositions in minerals (olivine and pyroxene), which are key in providing noble gas compositions of the magmatic source, especially when surface emissions are absent or difficult to access. Our new

1. Dipartimento DiSTeM, Università degli Studi di Palermo, Palermo, Italy
2. Istituto Nazionale di Geofisica e Vulcanologia, Sezione di Palermo, Palermo, Italy
3 Centro de Excelencia en Geotermia de los Andes (CEGA) y Departamento de Geología, Facultad de Ciencias Físicas y Matemáticas, Universidad de Chile, Santiago, Chile
4. Instituto Geológico Minero y Metalúrgico, Observatorio Vulcanológico del INGEMMET, Arequipa, Peru
* Corresponding author (email: joaopedro.nogueiralages@unipa.it)

helium data, integrated with noble gas data from other volcanic zones in the Andes, are used to resolve crustal *versus* slab controls on noble gas isotope variability along the arc.

Results

Our noble gas results derive from CO_2-dominated FIs trapped in olivine (Villarica, South Chile) and clinopyroxene (Peru) phenocrysts as gas (vapour) bubbles during and after magma crystallisation. The phenocrysts were handpicked from pyroclastic and scoria deposits at Villarica, and ballistic blocks and andesitic lava flows in Peru (Supplementary Information S-1). We focus on pyroxene in Peruvian volcanic products as, due to the more evolved nature of magmas produced along the CVZ, olivine is scarce and recurrently found in insufficient amounts for noble gas analyses. We followed identical sample preparation and analytical procedures to those described in Lages *et al.* (2021) for bulk element and isotope composition measurements of noble gases in each sample.

Despite low helium concentrations in Peruvian phenocrysts ($0.38–1.29 \times 10^{-13}$ mol/g), we obtain consistent results for Sabancaya, Ubinas, and El Misti volcanoes. The maximum observed $^3He/^4He$ ratios range from 5.9 (±0.2) to 6.4 (±0.2) R_A (Table S-1). As for Villarica, we measure similar helium concentrations in olivine (only as high as 1.27×10^{-13} mol/g). Both samples analysed yield comparable R_C/R_A values (6.5 ± 0.1 and 6.7 ± 0.1; Table S-1), below the MORB range, yet significantly higher than that reported in Hilton *et al.* (1993) of 4.3 ± 0.8 R_A.

An Improved Catalogue for Light Noble Gases in Andean Fluids

Our new data (Table S-1) fill an information gap in the central and southern volcanic zones of the Andes and are interpreted in the context of a noble gas compilation (Table S-2) we assembled from published noble gas studies on quaternary volcanic centres along the arc.

In their global arc compilation, Hilton *et al.* (2002) listed 81 samples (predominantly <100 °C) with available $^3He/^4He$ information for the Andes (117 in Sano and Fischer, 2013). Our updated catalogue (Supplementary Information S-2) now includes a total of 261 gas samples, with a significantly higher representation of fluid inclusion data analysis. However, and despite the significant increase in the number of samples available (including for other noble gases such as Ar and Ne), the overall dataset remains predominantly dominated (>60 % of the total; Fig. 1) by low temperature (<100 °C) gas emissions. This reflects (i) the difficulty of accessing volcano summits where high temperature fumaroles are typically concentrated, and (ii) the widespread occurrence of more accessible, peripheral manifestations (bubbling springs, steaming grounds, diffuse degassing) in volcano surroundings. Unfortunately, these are recurrently affected by secondary processes, including dilution of "magmatic" fluids by atmospheric/crustal He that ultimately lowers the pristine $^3He/^4He$ ratio (*e.g.*, gas manifestations at 0–100 °C and >3 km distance from the volcanic centre exhibit the lowest $^3He/^4He$ ratios on average; Fig. 1).

To overcome these limitations, recent studies have focused on the analysis of olivine- and pyroxene-hosted FIs found in lavas and pyroclastic deposits from active Andean volcanoes lacking noble gas information (*e.g.*, Robidoux *et al.*, 2020). Consequently, our novel data reported here for Ubinas, El Misti, and Sabancaya (Peru, CVZ), where surface gases have traditionally been challenging to measure (due to high level of activity at the open vents), delivers the first characterisation of noble gas signatures in the region. These, alongside our new noble gas results for Villarica (SVZ), provide the most thorough analysis of helium isotope compositions along the Andean volcanic arc.

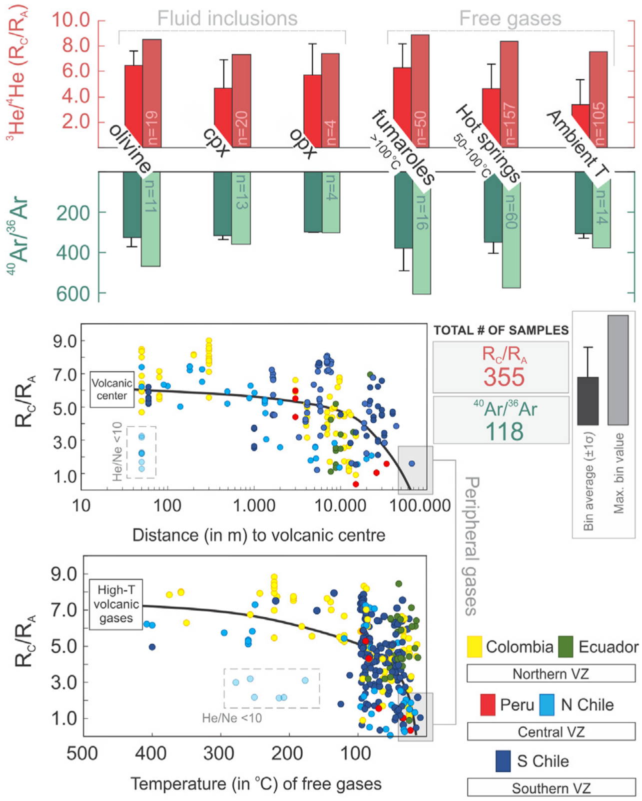

Figure 1 Distribution of helium and argon isotopic data (averages and maximum values) *per* sample category. Bottom: relation between R_C/R_A data in free gases, their sampling temperature, and distance to respective volcanic centres (Table S-2).

Exploring the Catalogue: Surface Gases *vs.* Fluid Inclusions

Our updated Andean dataset (Table S-2) benefits from the significant addition of FIs data to a yet gas-dominated compilation. More importantly, it ensures significant representability of three Andean arc segments (NVZ, CVZ and SVZ), and especially of some of their current most active volcanoes.

FIs account for only ~12 % of the helium dataset (Fig. 1). While Ne and Ar exhibit large proportions of atmospheric components, FIs generally exhibit higher $^3He/^4He$ ratios than surface gases. Figure 2 explores the $^3He/^4He$ populations of three Andean segments, and finds that (with the notable exception of Galeras; Sano *et al.*, 1997) FIs yield higher R/R_A values than surface gases. Therefore, although FIs can potentially be affected by post-entrapment ^3He and ^4He in growth and diffusion controlled isotope fractionation, their $^3He/^4He$ signatures offer the most faithful record of pristine magmatic source compositions. Our inferred magmatic end member compositions are shown in Figure 2, as derived from using the maximum R_C/R_A values for each arc segment. These are used below to interpret variations of $^3He/^4He$ signature in the mantle source along the arc.

Subducting Slab or Continental Crust?

Accepting our segment maximum R_C/R_A values (Fig. 2) as the most representative of the Andean magmatic source(s) (*e.*

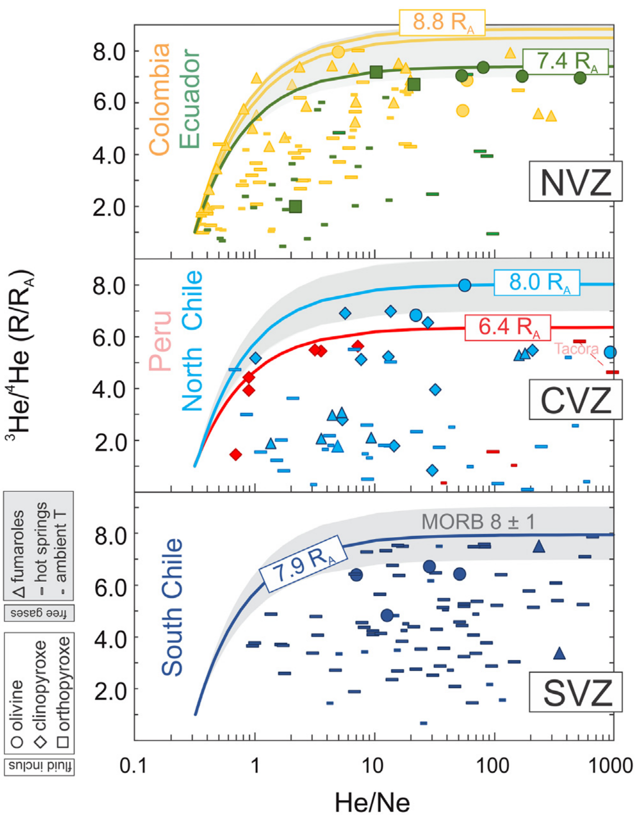

Figure 2 $^3He/^4He$ *vs* $^4He/^{20}Ne$ data in FIs and free gases. Binary mixing (air-magmatic end member) curves calculated with maximum R_C/R_A values for each segment.

g., as those least affected by secondary processes), we find little evidence of radiogenic contributions in Colombia and North/South Chile, in which the magmatic end members yield MORB-like values. However, more radiogenic $^3He/^4He$ ratios are observed in Ecuador and Peru (Fig. 2). Our goal below is to address if the drivers of these along arc variations operate (i) deep in the mantle source (*via* the subducting slab), or (ii) in the crust during magma ascent/storage.

Slab sediments are known as effective U and Th carriers (*e.g.*, Kelley *et al.*, 2005), and the fluids/melts they form by dehydration/melting (Skora *et al.*, 2015) may in principle lead to substantial radiogenic ^4He production (with a consequent $^3He/^4He$ ratio decrease) in the overriding mantle (Robidoux *et al.*, 2017). We test the possible role of recycled subducting sediments using the Th/La ratio slab proxy (Supplementary Information S-4; Plank, 2005). The ratio between these fluid-immobile elements is typically low in MORBs (<0.1), elevated in the continental crust (>0.25), and varies in arc basalts (~0.1–0.4) depending on the composition of sediments subducted at the corresponding trenches.

Plank (2005) demonstrates, for margins with high sediment fluxes (>0.32 Mg/yr/cm length), a correlation between Th/La in arc rocks and subducting sediments at corresponding trench. North and South Chile are the only Andean margins that fall in the high sediment flux category (0.53 and 0.55 Mg/yr/cm length, respectively), and their rock/sediment Th/La association consistently plot along the global array of Plank (2005), suggesting effective transfer of sediment-derived fluids to arc magmas in these regions (Fig. 3a, Table S-3). By contrast, Colombia, Ecuador and Peru, all low flux segments, exhibit a large spread in bulk volcanic rock Th/La compositions and $^3He/^4He$ ratios, and no obvious correlation with sediment Th/La (Fig. 3a).

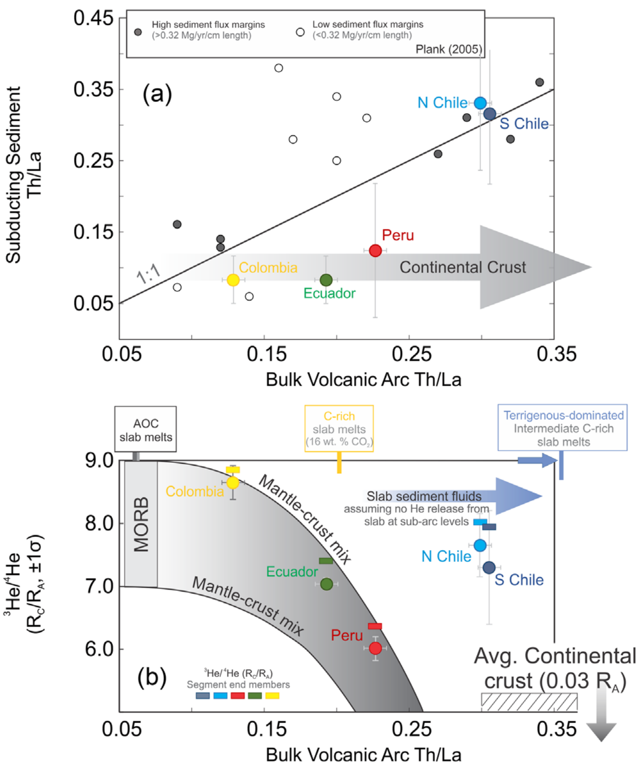

Figure 3 **(a)** Average Th/La in subducting sediments and volcanic arcs (Plank, 2005). For Andean segments, bulk sediment and arc compositions (Table S-3) are derived from Plank (2014) and the Andean GEOROC dataset, respectively (see Supplementary Information S-4). **(b)** $^3He/^4He$ averages and end members (this work) *vs.* bulk Th/La compositions of respective segments; the grey area indicates a binary mixing line between MORB and continental crust.

Instead, the Th/La *vs.* $^3He/^4He$ ratios association (Fig. 3b) is more consistent with the involvement of crustal fluids in the latter segments. We cannot exclude however, based on the results of Figure 3b, that the ~1 R_A difference between Colombia (8.5 and 8.8 R_A) and North/South Chile (7.9 and 8.0 R_A, high Th/La ratios of ~0.33 and 0.32, respectively; Fig. 3b; Tables S-3, S-4; Plank, 2014) is, at least partially, due to a higher U-Th slab recycling *via* subduction of sediments in the latter segment.

From Ballentine and Burnard (2002) the production rate of radiogenic ^4He from U and Th decay in the mantle wedge can be calculated as:

$$^4\text{He atoms g}^{-1}\,\text{yr}^{-1} = (3.115\times10^6 + 1.272\times10^5)\,[\text{U}] + 7.710\times10^5\,[\text{Th}]$$

where [U] and [Th] correspond to the abundance of these elements in terrigenous products subducted in the region (Plank, 2014; Table S-3). Additionally, we assume (i) mantle ^4He concentrations in the same range of those measured in gas-rich fluid inclusions from Andean products (*e.g.*, Ecuador; $\times10^{-12}$ mol/g; Lages *et al.*, 2021), and (ii) a mantle end member derived from the highest $^3He/^4He$ ratios measured in FIs (8.5 R_A, Nevado del Ruiz; Lages *et al.*, 2021). From these, we estimate that in 10 kyr enough radiogenic ^4He would be produced to lower the helium isotope signature of the underlying mantle wedge toward North/South Chile end member values. This estimate is similar to the time length of slab dehydration and mantle wedge contamination happening *via* sediment melts transported in the slab (Plank, 2005).

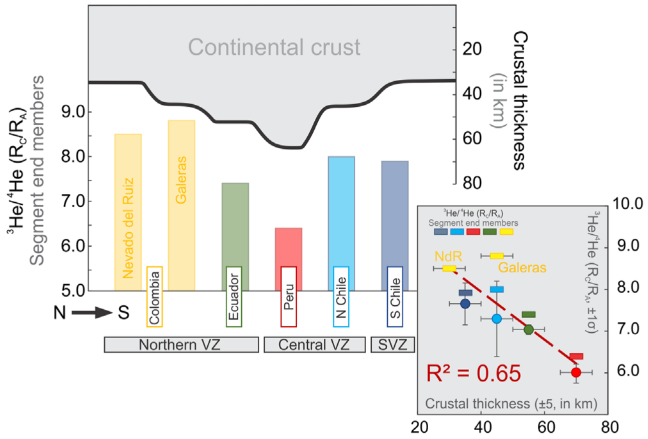

Figure 4 Crustal thickness variations along the Andes (transect); bottom, $^3He/^4He$ end members of respective arc segments (Fig. 2). Inset: co-variation of He isotopic signatures (avg. ±1σ, and end members) and crustal thicknesses at the arc scale; due to the crustal thickness anomaly detected at Nevado del Ruiz, the latter and Galeras are plotted separately.

We next test the hypothesis of a primary crustal control on the observed along arc variations in $^3He/^4He$ signatures, by matching these with the regional changes in crustal thickness (*e.g.*, Assumpção *et al.*, 2013; Fig. 4). On the south to north transect (Fig. 4), MORB-like helium isotope ratios are initially observed in North (CVZ) and South Chile (SVZ; 8.0 and 7.9 R_A, respectively), where the crust is 45–30 km thick. In the Peruvian Central Volcanic Zone, the more radiogenic He signature corresponds to the area where the crust is the thickest (>70 km). In this sector, all $^3He/^4He$ values obtained for Sabancaya, El Misti and Ubinas are <6.5 R_A and show low inter-variability. In Ecuador, we find both an increase in $^3He/^4He$ ratios (~7.4 R_A), and a decrease in crustal thickness (~50 km). The latter remains roughly constant up to the south of Colombia (~45 km), where in Galeras values as high as 8.8 R_A in fumarolic gases were reported by Sano *et al.* (1997). However, further north, crustal thickness decreases to ~35 km below Nevado del Ruiz and olivine-hosted FIs record $^3He/^4He$ values amongst the highest ever recorded in arc volcanism (8.5 R_A).

A co-variation between $^3He/^4He$ signatures and crustal thickness shows significant correlation at the scale of the entire arc (see inset Fig. 4). From this, we propose that the addition of radiogenic crustal ^4He to magma ascending through (being stored within) U-Th-rich crustal lithotypes are the main control factor on fluid $^3He/^4He$ signatures of continental arc volcanoes (Fig. 4). The unequivocal correlation we bring to light for most of the Andes further underlines the sensitivity of He isotopes in identifying and assessing crustal contamination processes. This correlation must be tested at arc scale in other subduction zones globally, as a more relevant role of the slab can be anticipated in regions where terrigenous sediments dominate the subducting input.

Acknowledgments

Two reviewers substantially improved this paper and are gratefully acknowledged. We thank Marco Rivera (OVI-INGEMMET) for his support during fieldwork in Peru and Aaron Sancho for his work on Chaillupén samples (Villarica). INGV-Palermo provided the analytical facilities. We thank Mariano Tantillo and Mariagrazia Misseri for their support in sample preparation and noble gas analysis. The fieldwork portion of this work was funded by the DECADE initiative, from the Deep Carbon Observatory - Alfred P. Sloan Foundation. This study also received funding from Miur under grant PRIN2017-2017LMNLAW.

Editor: Maud Boyet

Additional Information

Supplementary Information accompanies this letter at https://www.geochemicalperspectivesletters.org/article2134.

Cite this letter as: Lages, J., Rizzo, A.L., Aiuppa, A., Robidoux, P., Aguilar, R., Apaza, F., Masias, P. (2021) Crustal controls on light noble gas isotope variability along the Andean Volcanic Arc. *Geochem. Persp. Let.* 19, 45–49.

References

Aiuppa, A., Fischer, T.P., Plank, T., Robidoux, P., Di Napoli, R. (2017) Along-arc, inter-arc and arc-to-arc variations in volcanic gas CO_2/S_T ratios reveal dual source of carbon in arc volcanism. *Earth-Science Reviews* 168, 24–47.

Ancellin, M.-A., Samaniego, P., Vlastelic, I., Nauret, F., Gannoun, A., Hidalgo, S. (2017) Across-arc versus along-arc Sr-Nd-Pb isotope variations in the Ecuadorian volcanic arc. *Geochemistry Geophysics Geosystems* 18, 1163–1188.

Assumpção, M., Feng, M., Tassara, A., Julià, J. (2013) Models of crustal thickness for South America from seismic refraction, receiver functions and surface wave tomography. *Tectonophysics* 609, 82–96.

Ballentine, C.J., Burnard, P.G. (2002) Production, release and transport of noble gases in the continental crust. *Reviews in Mineralogy and Geochemistry* 47, 481–538.

Graham, D.W. (2002) Noble gas isotope geochemistry of mid-ocean ridge and ocean island basalts: Characterization of mantle source reservoirs. *Reviews in Mineralogy and Geochemistry* 47, 247–317.

Hanan, B.B., Graham, D.W. (1996) Lead and Helium Isotope Evidence from Oceanic Basalts for a Common Deep Source of Mantle Plumes. *Science* 272, 991–995.

Hidalgo, S., Gerbe, M.C., Martin, H., Samaniego, P., Bourdon, E. (2012) Role of crustal and slab components in the Northern Volcanic Zone of the Andes (Ecuador) constrained by Sr-Nd-O isotopes. *Lithos* 132–133, 180–192.

Hilton, D.R., Hammerschmidt, K., Teufel, S., Friedrichsen, H. (1993) Helium isotope characteristics of Andean geothermal fluids and lavas. *Earth and Planetary Science Letters* 120, 265–282.

Hilton, D.R., Fischer, T.P., Marty, B. (2002) Noble gases and volatile recycling at subduction zones. *Reviews in Mineralogy and Geochemistry* 47, 319–370.

Kagoshima, T., Sano, Y., Takahata, N., Maruoka, T., Fischer, T.P., Hattori, K. (2015) Sulphur geodynamic cycle. *Scientific Reports* 5, 8330.

Kelley, K.A., Plank, T., Farr, L., Ludden, J., Staudigel, H. (2005) Subduction cycling of U, Th, and Pb. *Earth and Planetary Science Letters* 234, 369–383.

Lages, J., Rizzo, A.L., Aiuppa, A., Samaniego, P., Le Pennec, J.L., Ceballos, J.A., Narváez, P.A., Moussallam, Y., Bani, P., Schipper, C.I., Hidalgo, S., Gaglio, V., Alberti, E., Sandoval-Velasquez, A. (2021) Noble gas magmatic signature of the Andean Northern Volcanic Zone from fluid inclusions in minerals. *Chemical Geology* 559, 119966.

Mamani, M., Wörner, G., Sempere, T. (2010) Geochemical variations in igneous rocks of the Central Andean orocline (13°S to 18°S): Tracing crustal thickening and magma generation through time and space. *GSA Bulletin* 122, 162–182.

Mason, E., Edmonds, M., Turchyn, A.V. (2017) Remobilization of crustal carbon may dominate volcanic arc emissions. *Science* 357, 290–294.

Plank, T. (2005) Constraints from Thorium/Lanthanum on sediment recycling at subduction zones and the evolution of the continents. *Journal of Petrology* 46, 921–944.

Plank, T. (2014) 4.17 - The Chemical Composition of Subducting Sediments. In: Holland, H.D., Turekian, K.K. (Eds.) *Treatise on Geochemistry*. Second Edition, Elsevier, Oxford, 607–629.

Poreda, R., Craig, H. (1989) Helium isotopes ratios in circum-Pacific volcanic arcs. *Nature* 338, 473–478.

Robidoux, P., Aiuppa, A., Rotolo, S.G., Rizzo, A.L., Hauri, E.H., Frezzotti, M.L. (2017) Volatile contents of mafic-to-intermediate magmas at San Cristóbal volcano in Nicaragua. *Lithos* 272–273, 147–163.

Robidoux, P., Rizzo, A.L., Aguilera, F., Aiuppa, A., Artale, M., Liuzzo, M., Nazzari, M., Zummo, F. (2020) Petrological and noble gas features of Lascar and Lastarria volcanoes (Chile): Inferences on plumbing systems and mantle characteristics. *Lithos* 370–371, 105615.

Sano, Y., Fischer, T.P. (2013) The analysis and interpretation of noble gases in modern hydrothermal systems. In: Burnard P. (Ed.) *The Noble Gases as Geochemical Tracers*. Springer, Berlin, Heidelberg, 249–317.

Sano, Y., Gamo, T., Williams, S.N. (1997) Secular variations of helium and carbon isotopes at Galeras volcano, Colombia. *Journal of Volcanology and Geothermal Research* 77, 255–265.

Skora, S., Blundy, J.D., Brooker, R.A., Green, E.C.R., de Hoog, J.C.M., Connolly, J. A.D. (2015) Hydrous phase relations and trace element partitioning behaviour in calcareous sediments at subduction-zone conditions. *Journal of Petrology* 56, 953–980.

Stern, C.R. (2004) Active Andean Volcanism. *Andean Geology* 31, 161–206.

Syracuse, E.M., van Keken, P.E., Abers, G.A., Suetsugu, D., Bina, C., Inoue, T., Wiens, D., Jellinek, M. (2010) The global range of subduction zone thermal models. *Physics of the Earth and Planetary Interiors* 183, 73–90.

Zellmer, G.F., Edmonds, M., Straub, S.M. (2015) Volatiles in subduction zone magmatism. *Geological Society, London, Special Publications* 410, 1–17.

Geochemical Perspectives Letters

Crustal controls on isotope variability of light noble gases along the Andean Volcanic Arc

J. Lages, A.L. Rizzo, A. Aiuppa, P. Robidoux,
R. Aguilar, F. Apaza, P. Masias

Supplementary Information

The Supplementary Information includes:

S-1 New Isotope Results and Noble Gas Abundances (Peru and S Chile)

Brief Petrological Descriptions of Volcanoes Sampled in This Study

Sabancaya (Peru, CVZ)

The Ampato–Sabancaya volcanic complex comprises two successive edifices. During the Holocene, eruptive activity migrated to the NE and built up the Sabancaya edifice, between 6 and 3 ka. This cone comprises andesitic and dacitic blocky lava flows emplaced during at least two eruptive stages (Samaniego *et al*., 2016). The Ampato–Sabancaya rocks display a high-K magmatic affinity and range from andesites to dacites (57–69 wt. % SiO_2), with rare rhyolitic compositions (74–77 wt. % SiO_2). We analysed two lava samples from the Sabancaya basal edifice (3 ± 5 ka; Samaniego *et al*., 2016) that present porphyritic texture, composed of phenocrysts (30–60 vol. %) of plagioclase, biotite, amphibole, clinopyroxene, Fe-Ti oxides, and eventually by orthopyroxene and olivine (<2 %; Samaniego *et al*., 2016). The FIs analysed from noble gases in this study were entrapped in clinopyroxene host minerals (Table S-1).

Ubinas (Peru, CVZ)

Over the past 500 years, Ubinas produced mostly tephra with a trend towards more mafic magma compositions in recent times (Thouret *et al*., 2005). The 2006 and 2014 juvenile blocks here analysed are dark to grey, dense to poorly vesicular, porphyritic andesites bearing 20–25 vol. % phenocrysts (300 μm to 1.8 mm), 30–40 vol. % microphenocrysts (100–300 μm), and 35–50 vol. % matrix glass. Phenocrysts of plagioclase, clinopyroxene, orthopyroxene, and Fe-Ti oxides are abundant. Both samples show a similar mineral assemblage including plagioclase, clinopyroxene, orthopyroxene, and magnetite with scarce amphibole and olivine (Rivera *et al*., 2014). Olivine phenocrysts occur in the 2006 ballistic blocks, although not in sufficient amounts for FIs analysis of noble gases.

El Misti (Peru, CVZ)

El Misti is a major andesitic volcano located near the city of Arequipa in the northern Central Volcanic Zone. Plagioclase is by far the most abundant mineral phase followed in order of abundance by amphibole and pyroxene. Olivine occurs only in mafic andesites and when present is scarce, never exceeding 2 vol. %. Rivera *et al*. (2017) report on subhedral to anhedral olivine crystals with sizes smaller than 400 μm for Misti 2 lava flows from which both samples in this study were collected (112–40 ka), with forsterite composition of $Fo_{76–80}$. When compared with olivines from primitive arc magmas (Fo_{80}), the relatively low-Fo content of the El Misti olivine ($Fo_{70–80}$) provides evidence against a pure, primary, mantled-derived origin for El Misti rocks (Rivera *et al*., 2017).

Villarrica (CSVZ, South Chile)

Activity at Villarrica has been characterised in the past by frequent small eruptions as well as highly explosive, caldera-forming pyroclastic eruptions of mainly basaltic andesite magma (Moreno and Clavero, 2006). Samples collected for analysis included scoria samples from the 3 March 2015 paroxysmal eruption (Aiuppa *et al*., 2017), with Fo contents ranging from about 70 to 82 % (avg. 77 %). Previously analysed samples representing the magma filling the central crater were determined to hold 33 wt. % plagioclase ($An_{58–74}$), 7 wt. % olivine ($Fo_{75–78}$), and trace amounts of chromian spinel (Witter *et al*., 2004). The other sample analysed (HCH2A1; Sancho, 2019) is taken from a ~100-m-high adventitious eruptive centre from the sub-group 2 of Chaillupén hch2 (<3.7 ka; Moreno and Clavero, 2006). The rock represents a ballistic projectile taken on the crater rim of a pyroclastic cone, ubicated downhill at the southern end of the N–S fracture that cuts through Villarrica's south flank. The rock sample is characterised as a fine-grained, dense fusiform bomb-size pyroclast of mafic composition with 20 vol. % plagioclase, 6 vol. % clinopyroxene, 4 vol. % olivine as determined from thin section analysis.

Table S-1 Noble gas abundances and isotope compositions in fluid inclusions (Peru and S Chile).

Volcano	Sample ID	Sample details	Rock[a]	Min. phase[b]	[He][c] ×10^{-13}	[Ne][c] ×10^{-17}	[^{40}Ar][c] ×10^{-12}	[^{36}Ar][c] ×10^{-15}	[^{40}Ar*][c] ×10^{-13}	^{4}He/^{20}Ne	^{20}Ne/^{22}Ne	^{21}Ne/^{22}Ne	^{4}He/^{40}Ar*	^{40}Ar/^{36}Ar	^{3}He/^{4}He (R/R$_A$)	^{3}He/^{4}He (R$_C$/R$_A$)	$CO_2/^3He$[c] ×10^{-9}
South Chile (SVZ)																	
Villarrica	2015_B	Scoria	BA	Ol	1.27	2.50	6.15	20.38	1.24	50.8	9.83 ± 0.03	0.0295 ± 0.0005	1.02	301.6 ± 0.1	6.43	6.46 ± 0.12	0.013
	HCH2A1	Pyroclast (bomb)	BA	Ol	0.72	10.32	1.03	3.40	0.21	7.0	9.81 ± 0.02	0.0293 ± 0.0003	3.39	301.8 ± 0.7	6.39	6.66 ± 0.13	0.627
Peru (CVZ)																	
Ubinas	2014	Juvenile blocks	A	Cpx	0.72	9.86	6.95	19.75	11.19	7.3	9.67 ± 0.02	0.0284 ± 0.0003	0.06	352.2 ± 0.8	5.64	5.86 ± 0.16	16.461
	2016 A & B	Juvenile blocks	A	Cpx	1.29	39.69	15.27	48.72	8.75	3.2	9.66 ± 0.02	0.0285 ± 0.0002	0.15	313.5 ± 0.04	5.49	6.01 ± 0.16	7.203
Sabancaya	SA-09-11	Lava flow	A	Cpx	0.38	10.63	0.71	1.98	1.27	3.6	9.67 ± 0.03	0.0288 ± 0.0004	0.30	359.7 ± 0.2	5.45	5.92 ± 0.23	0.484
	SA-09-17	Lava flow	A	Cpx	0.08	12.57	0.93	2.92	0.70	0.7	9.77 ± 0.01	0.0292 ± 0.0003	0.12	319.4 ± 0.1	1.45	2.11 ± 0.18	16.460
El Misti	Misti 2 (A)	Lava flow	A	Cpx	1.19	2.18	4.16	1.35	1.82	0.9	9.89 ± 0.01	0.0289 ± 0.00031	0.08	309.0 ± 0.06	3.93	5.80 ± 0.177	–
	Misti 2 (B)	Lava flow	A	Cpx	0.78	1.31	4.84	1.56	2.32	0.9	9.84 ± 0.01	0.0297 ± 0.00019	0.12	310.4 ± 0.06	4.43	6.36 ± 0.190	–

[a] Host rock chemical classification on the basis of SiO_2 content: A, andesite; BA, basaltic-andesite.

[b] Mineral phases analysed: Ol, olivine; Cpx, clinopyroxene.

[c] Noble gas and CO_2 concentrations in mol g^{-1}.

S-2 Data References, Dataset Description, and Full Data Table (with Table Guide)

The data table below includes He, Ar, and Ne data available for quaternary volcanoes from the Andean Volcanic Arc. Noble gas data reported for amagmatic regions of the arc (*e.g.*, flat-slab segments) have not been included (see Simmons *et al*., 1987; Hoke *et al*., 1994; Hoke and Lamb, 2007; Newell *et al*., 2015).

S-2.1 Catalogue References (in Table S-2)

1. Williams, S.N., Sano, Y., Wakita, H. (1987) Helium-3 emission from Nevado Del Ruiz Volcano, Colombia. *Geophysical Research Letters* 10, 1035–1038.

2. Sano, Y., Wakita, H., Williams, S.N. (1990) Helium-isotope systematics at Nevado del Ruiz volcano, Colombia: implications for the volcanic hydrothermal system. *Journal of Volcanology and Geothermal Research* 42, 41–52.

3. Lages, J., Rizzo, A.L., Aiuppa, A., Samaniego, P., Le Pennec, J.L., Ceballos, J.A., Narváez, P.A., Moussallam, Y., Bani, P., Schipper, C.I., Hidalgo, S., Gaglio, V., Alberti, E., Sandoval-Velasquez, A. (2021) Noble gas magmatic signature of the Andean Northern Volcanic Zone from fluid inclusions in minerals. *Chemical Geology* 559, 119966.

4. Sturchio, N.C., Williams, S.N., Sano, Y. (1993) The hydrothermal system of Volcan Puracé, Colombia. *Bulletin of Volcanology* 55, 289–296.

5. Maldonado, L.F.M., Inguaggiato, S., Jaramillo, M.T., Valencia, G.G., Mazot, A. (2017) Volatiles and energy released by Puracé volcano. *Bulletin of Volcanology* 79, 84.

6. Sano, Y., Williams, S.N. (1996) Fluxes of mantle and subducted carbon along convergent plate boundaries. *Geophysical Research Letters* 23, 2749–2752.

7. Sano, Y., Gamo, T., Williams, S.N. (1997) Secular variations of helium and carbon isotopes at Galeras volcano, Colombia. *Journal of Volcanology and Geothermal Research* 77, 255–265.

8. Inguaggiato, S., Londoño, J.M., Chacón, Z., Liotta, M., Gil, E., Alzate, D. (2017) The hydrothermal system of Cerro Machín volcano (Colombia): New magmatic signals observed during 2011–2013. *Chemical Geology* 469, 60–68.

9. Lewicki, J.L., Fischer, T., Williams, S.N. (2000) Chemical and isotopic compositions of fluids at Cumbal Volcano, Colombia: Evidence for magmatic contribution. *Bulletin of Volcanology* 62, 347–361.

10. Fischer, T.P., Sturchio, N.C., Stix, J., Arehart, G.B., Counce, D., Williams, S.N. (1997) The chemical and isotopic composition of fumarolic gases and spring discharges from Galeras Volcano, Colombia. *Journal of Volcanology and Geothermal Research* 77, 229–253.

11. Inguaggiato, S., Hidalgo, S., Beate, B., Bourquin, J. (2010) Geochemical and isotopic characterization of volcanic and geothermal fluids discharged from the Ecuadorian volcanic arc. *Geofluids* 10, 525–541.

12. Hilton, D.R., Hammerschmidt, K., Teufel, S., Friedrichsen, H. (1993) Helium isotope characteristics of Andean geothermal fluids and lavas. *Earth and Planetary Science Letters* 120, 265–282.

13. Inostroza, M., Tassi, F., Aguilera, F., Sepúlveda, J.P., Capecchiacci, F., Venturi, S., Capasso, G., 2020. Geochemistry of gas and water discharge from the magmatic-hydrothermal system of Guallatiri volcano, northern Chile. *Bulletin of Volcanology* 82, 57.

14. Lopez, T., Aguilera, F., Tassi, F., Maarten de Moor, J., Bobrowski, N., Aiuppa, A., Tamburello, G., Rizzo, A.L., Liuzzo, M., Viveiros, F., Cardellini, C., Silva, C., Fischer, T., Jean-Baptiste, P., Kazayaha, R., Hidalgo, S., Malowany, K., Lucic, G., Bagnato, E., Bergsson, B., Reath, K., Liotta, M., Carn, S., Chiodini, G. (2018) New insights into the magmatic-hydrothermal system and volatile budget of Lastarria volcano, Chile: Integrated results from the 2014 IAVCEI CCVG 12th Volcanic Gas Workshop. *Geosphere* 14, 983–1007.

15. Aguilera, F., Tassi, F., Darrah, T., Moune, S., Vaselli, O. (2012) Geochemical model of a magmatic-hydrothermal system at the Lastarria volcano, northern Chile. *Bulletin of Volcanology* 74, 119–134.

16. Tassi, F., Aguilera, F., Vaselli, O., Medina, E., Tedesco, D., Delgado Huertas, A., Poreda, R., Kojima, S. (2009) The magmatic- and hydrothermal-dominated fumarolic system at the Active Crater of Lascar volcano, northern Chile. *Bulletin of Volcanology* 71, 171–183.

17. Tassi, F., Aguilera, F., Vaselli, O., Darrah, T., Medina, E. (2011) Gas discharges from four remote volcanoes in northern Chile (Putana,Olca, Irruputuncu and Alitar): A geochemical survey. *Annals of Geophysics* 54, 121–136.

18. Roulleau, E., Tardani, D., Sano, Y., Takahata, N., Vinet, N., Bravo, F., Muñoz, C., Sanchez, J. (2016) New insight from noble gas and stable isotopes of geothermal/hydrothermal fluids at Caviahue-Copahue Volcanic Complex: Boiling steam separation and water-rock nteraction at shallow depth. *Journal of Volcanology and Geothermal Research* 328, 70–83.

19. Tassi, F., Aguilera, F., Benavente, O., Paonita, A., Chiodini, G., Caliro, S., Agusto, M., Gutierrez, F., Capaccioni, B., Vaselli, O., Caselli, A., Saltori, O. (2016) Geochemistry of fluid discharges from Peteroa volcano (Argentina-Chile) in 2010–2015: Insights into compositional changes related to the fluid source region(s). *Chemical Geology* 432, 41–53.

20. Agusto, M., Tassi, F., Caselli, A.T., Vaselli, O., Rouwet, D., Capaccioni, B., Caliro, S., Chiodini, G., Darrah, T. (2013) Gas geochemistry of the magmatic-hydrothermal fluid reservoir in the Copahue-Caviahue Volcanic Complex (Argentina). *Journal of Volcanology and Geothermal Research* 257, 44–56.

21. Robidoux, P., Rizzo, A.L., Aguilera, F., Aiuppa, A., Artale, M., Liuzzo, M., Nazzari, M., Zummo, F. (2020) Petrological and noble gas features of Lascar and Lastarria volcanoes (Chile): Inferences on plumbing systems and mantle characteristics. *Lithos* 370–371, 105615.

22. Benavente, O., Tassi, F., Reich, M., Aguilera, F., Capecchiacci, F., Gutiérrez, F., Vaselli, O., Rizzo, A. (2016) Chemical and isotopic features of cold and thermal fluids discharged in the Southern Volcanic Zone between 32.5°S and 36°S: Insights into the physical and chemical processes controlling fluid geochemistry in geothermal systems of Central Chile. *Chemical Geology* 420, 97–113.

23. Ray, M.C., Hilton, D.R., Muñoz, J., Fischer, T.P., Shaw, A.M. (2009) The effects of volatile recycling, degassing and crustal contamination on the helium and carbon geochemistry of hydrothermal fluids from the Southern Volcanic Zone of Chile. *Chemical Geology* 266, 38–49.

24. Tardani, D., Reich, M., Roulleau, E., Takahata, N., Sano, Y., Pérez-Flores, P., Sánchez-Alfaro, P., Cembrano, J., Arancibia, G. (2016) Exploring the structural controls on helium, nitrogen and carbon isotope signatures in hydrothermal fluids along an intra-arc fault system. *Geochimica et Cosmochimica Acta* 184, 193–211.

25. Capaccioni, B., Aguilera, F., Tassi, F., Darrah, T., Poreda, R.J., Vaselli, O. (2011) Geochemical and isotopic evidences of magmatic inputs in the hydrothermal reservoir feeding the fumarolic discharges of Tacora volcano (northern Chile). *Journal of Volcanology and Geothermal Research* 208, 77–85.

26. Benavente, O., Tassi, F., Gutiérrez, F., Vaselli, O., Aguilera, F., Reich, M. (2013) Origin of fumarolic fluids from Tupungatito Volcano (Central Chile): Interplay between magmatic, hydrothermal, and shallow meteoric sources. *Bulletin of Volcanology* 75, 1–15.

27. Hoke, L., Hilton, D.R., Lamb, S.H., Hammerschmidt, K., Friedrichsen, H. (1994) ^{3}He evidence for a wide zone of active mantle melting beneath the Central Andes. *Earth and Planetary Science Letters* 128, 341–355.

28. Tassi, F., Aguilera, F., Darrah, T., Vaselli, O., Capaccioni, B., Poreda, R.J., Delgado Huertas, A. (2010) Fluid geochemistry of hydrothermal systems in the Arica-Parinacota, Tarapacá and Antofagasta regions (northern Chile). *Journal of Volcanology and Geothermal Research* 192, 1–15.

S-2.2 Table Guidelines

The colours of the headlines throughout the noble gas catalogue table correspond to the colour scheme used in the figures to distinguish between the five different countries and their respective volcanic arc segments (NVZ, Colombia and Ecuador; CVZ, Peru and North Chile; SVZ, South Chile):

i) Lat and Long columns: "Lat" (latitude) and "Long" (longitude), when not provided, were estimated by name of sampling location and/or map figures showing sampling coordinates; values inferred appear in red in both columns. Note that FIs data are assigned the exact coordinates of the volcanic edifice of origin.

ii) Dist. (m) and Temp. (°C): Values for distance (Dist.) and temperature (Temp.), when not originally reported, were assigned based on sampling coordinates (for distance to the main volcanic centre) and previous temperatures reported for the same sampling location (for the temperature column), all in red. Samples with no temperature and/or distance information are due to insufficient information available to infer the sampling parameters. For hydrothermal samples not associated with a main volcanic system, the distance parameter results non-applicable (n/a).

iii) Type: The dataset is subdivided into the following sample types (see also Fig. 1 in the main text): 1, fluid inclusions (FIs) data in olivine phenocrysts; 2, FIs in clinopyroxene; 3, FIs in orthopyroxene; 4, free gases at >100 °C; 5, free gases at 50–100 °C; 6, free gases at <50 °C.

iv) Isotope ratios correction: Helium isotopic ratios reported in the form of R_C/R_A, where R_C is the air-corrected $^3He/^4He$ ratio of the sample, assessed based on $^4He/^{20}Ne$ ratios (also in table):

$$R_C/R_A = [(R_M/R_A)(He/Ne)_M - (He/Ne)_{air}]/[(He/Ne)_M - (He/Ne)_{air}],$$

where the subscripts "M" and "air" refer to measured and atmospheric theoretical values, respectively. Argon isotope ratios account for atmospheric-corrected ^{40}Ar, assuming that all ^{36}Ar contained in the gas phase is of atmospheric origin:

$$^{40}Ar^* = {}^{40}Ar_M - [(^{40}Ar/^{36}Ar)_{air} \times {}^{36}Ar_M],$$

where $^{40}Ar^*$ represents the corrected isotope value and M indicates the measured value.

v) err: Isotopic ratio errors are 1σ uncertainties.

Table S-2 Noble gas catalogue of the Andean Volcanic Arc.

Table S-2 is available for download (Excel) from the online version of the article at http://www.geochemicalperspectivesletters.org/article2134.

S-3 Neon and Argon Systematics of Andean Magmatic Fluids

In contrast to the extensive $^{3}He/^{4}He$ database described in the main text, there are relatively few $^{40}Ar/^{36}Ar$ samples (118) and even fewer $^{20}Ne/^{22}Ne$ and $^{21}Ne/^{22}Ne$ samples (34 and 33, respectively; Fig. S-1).

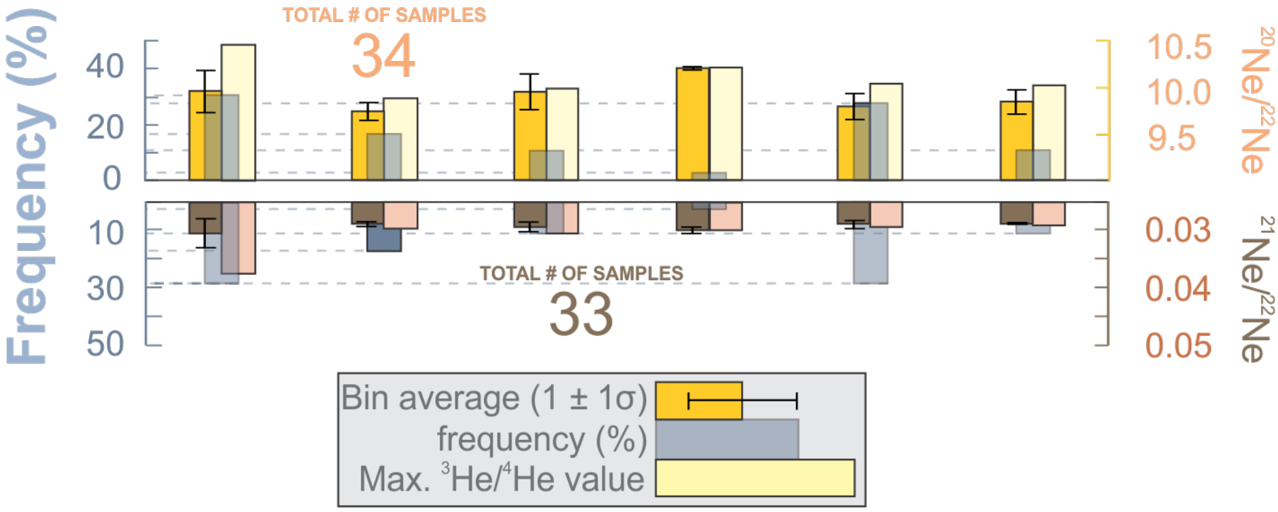

Figure S-1 Histogram of distribution, following those of Fig. 1 in the main text. Frequencies of the data type are shown on the left axis (faded columns; see Fig.1 in the main text for labels); averages (darker) and maximum values, per category, showed on the right axis.

Compared to intraplate and middle oceanic ridge environments, subduction-related fluids are known to carry larger proportions of atmospheric components (Burnard *et al.*, 1997), and Ar isotopes in FIs from volcanic arc rocks consistently show $^{40}Ar/^{36}Ar$ ratios close to the atmosphere (295.5; Hilton *et al.*, 2002). In our catalogue, the observed Andean gas-rocks $^{40}Ar/^{36}Ar$ ratios range from 287.5 to 610, but the arc average of ~339 (taken across all gas-rocks samples) denotes a close-to-atmospheric $^{40}Ar/^{36}Ar$ signature, well below that of MORB (~44,000; Moreira *et al.*, 1998). Similarly, neon isotopes (≤0.038 for $^{21}Ne/^{22}Ne$ and ≤10.46 for $^{20}Ne/^{22}Ne$) cluster at around the atmospheric ratios (0.029 and 9.8 for $^{21}Ne/^{22}Ne$ and $^{20}Ne/^{22}Ne$, respectively; Sarda *et al.*, 1988). These atmospheric Ar-Ne isotopic signatures imply variable (but substantial) degrees of contamination by an atmosphere-derived component that reflect their relatively large (compared to helium) air abundances (Hilton *et al.*, 2002; Fig. S-2). Notably, FIs also exhibit this atmospheric imprint: their Ne isotopic pairs and $^{40}Ar/^{36}Ar$ ratios (see histogram in Figs. 1 and S-1) are often lower than in high-temperature gases and comparable to those obtained from low-temperature emission sources. Recycling of atmosphere-derived Ar in the mantle, via dehydration of the subducting oceanic crust, has often been invoked (Matsumoto *et al.*, 2001; Hopp and Ionov, 2011; Di Piazza *et al.*, 2015; Rizzo *et al.*, 2016; Robidoux *et al.*, 2017, 2020; Battaglia *et al.*, 2018), although air contamination during surface rock exposure is often difficult to rule out.

Figure S-2 illustrates the binary trends of atmosphere-mantle mixing for both Argon and Neon isotopic ratios. Most importantly, our dataset indicates that atmosphere-derived components are still dominant even in FIs. Contrarily to the $^{3}He/^{4}He$ results, these show little difference when compared to argon and neon isotope results obtained in free gases, including those <100 °C (see Fig. 1 in the main text).

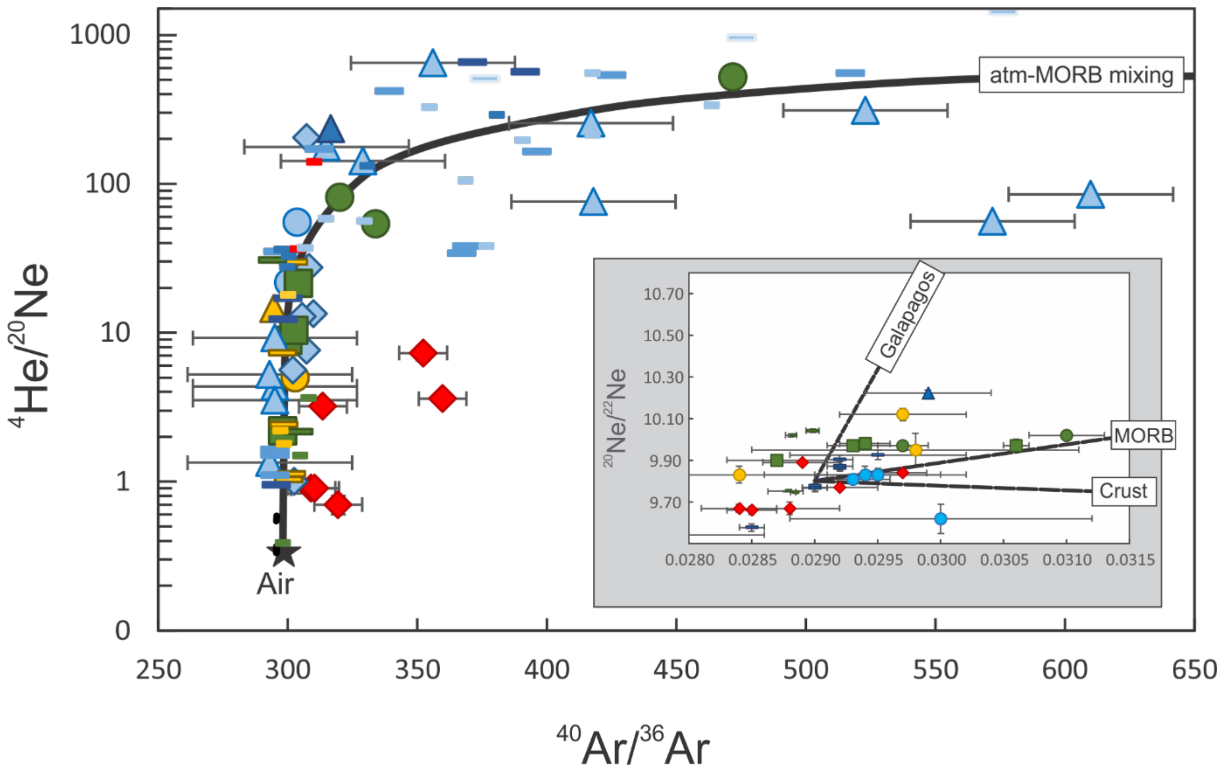

Figure S-2 Air-MORB mixing showing the extent of air contamination in samples from all categories (from FIs to low-temperature free gases); Inset: binary mixing between air and a MORB mantle as defined by Sarda *et al.* (1988) and Moreira *et al.* (1998) at ^{21}Ne/^{22}Ne = 0.06 and ^{20}Ne/^{22}Ne = 12.5; binary mixing between air and the OIB domain of the Galapagos Islands as determined by Kurz *et al.* (2009) at ^{21}Ne/^{22}Ne = 0.032 and ^{20}Ne/^{22}Ne = 12.5; crustal-neon trend from Kennedy *et al.* (1990).

S-4 Slab Constraints from Th/La in Sediments (Subducted) and Volcanic Products (Erupted) Along the Andean Volcanic Arc

To test the possible slab control on the ^{3}He/^{4}He signature of the mantle wedge along the Andes, we followed the approach of Plank (2005), who used the Th/La ratio as a tracer for the contribution of subducting sediments to arc magmas. This tracer is particularly useful since radiogenic ^{4}He mostly derives from the decay of natural U and Th series elements in rocks and sediments.

The author suggests that where little sediment subducts, arcs should have approximately mantle Th/La, whereas, in places with a high flux of subducted sediment, the Th/La of the arc should approach the sediment ratio. The latter varies with the proportions of terrigenous, hydrogenous and volcaniclastic sources. Th/La signatures in arc magmas should therefore provide information on the proportion of sediment to mantle, and therefore a way to calibrate the influence of sediment melts delivered by the slab at an arc-segment scale.

The Th/La data used in Figure 3a, b (main text) have been extracted from the 'GEOROC' (Geochemistry of Rocks of the Oceans and Continents) database (http://georoc.mpch-mainz.gwdg.de/georoc/Start.asp). The relevant data have been taken from the *'Precompiled Files/Locations/Convergent Margins'* files *'ANDEAN ARC part1.csv'* and *'ANDEAN ARC part2.csv'* that are freely available for download. The following tables summarise the available dataset.

Table S-3 Th/La data used in Figure 3a.

Volcanic products (GEOROC)			Sediments (Plank, 2014)		
Arc Segment	Bulk Arc Segment Th/La (avg.)*	1σ	Th/La	Th [ppm]	La [ppm]
Colombia	0.1007	0.0383	[1]0.083	1.21	14.6
Ecuador	0.1746	0.0464	[2]0.083	1.21	14.6
Peru	0.1723	0.1084	0.124	3.54	28.6
N Chile	0.2399	0.1133	0.332	5.08	15.3
S Chile	0.2177	0.1081	0.318	4.74	14.9

* Including only samples with <58 wt. % SiO_2.

[1,2] Th and La contents in sediments are averages for Colombia and Ecuador.

Table S-4 Th/La data used in Figure 3b.

GEOROC dataset				This review
Volcanic system	Avg Th/La of volcanic products	1σ	*N* samples	Maximum R_C/R_A
Nevado del Ruiz	0.2665	0.0798	4	8.46
Galeras	0.2953	0.0684	13	8.84
Cotopaxi	0.3099	0.1552	84	7.04
Tungurahua	0.3262	0.1183	89	7.40
El Reventador	0.1584	0.0182	15	6.98
Ubinas	0.1800	0.0344	14	6.01
El Misti	0.3462	0.2109	40	6.36
Sabancaya	0.2432	0.1303	14	5.92
Lascar	0.3160	0.1087	8	7.30
Lastarria	0.5908	0.1473	3	8.01
Villarica	0.1956	0.0694	10	6.66
Copahue	0.4165	0.0001	2	7.94

Supplementary Information References

Aiuppa, A., Bitetto, M., Francofonte, V., Velasquez, G., Parra, C.B., Giudice, G., Liuzzo, M., Moretti, R., Moussallam, Y., Peters, N., Tamburello, G., Valderrama, O.A., Curtis, A. (2017) A CO_2-gas precursor to the March 2015 Villarrica volcano eruption. *Geochemistry, Geophysics, Geosystems* 18, 2120–2132.

Battaglia, A., Bitetto, M., Aiuppa, A., Rizzo, A.L., Chigna, G., Watson, I.M., D'Aleo, R., Juárez Cacao, F.J., de Moor, M.J. (2018) The Magmatic Gas Signature of Pacaya Volcano, With Implications for the Volcanic CO_2 Flux from Guatemala. *Geochemistry, Geophysics, Geosystems* 19, 667–692.

Burnard, P., Graham, D., Turner, G. (1997) Vesicle-specific noble gas analyses of "popping rock": Implications for primordial noble gases in earth. *Science* 276, 568–571.

Di Piazza, A., Rizzo, A.L., Barberi, F., Carapezza, M.L., De Astis, G., Romano, C., Sortino, F. (2015) Geochemistry of the mantle source and magma feeding system beneath Turrialba volcano, Costa Rica. *Lithos* 232, 319–335.

Hilton, D.R., Fischer, T.P., Marty, B. (2002) Noble gases and volatile recycling at subduction zones. *Reviews in Mineralogy and Geochemistry* 47, 319–370.

Hoke, L., Lamb, S. (2007) Cenozoic behind-arc volcanism in the Bolivian Andes, South America: implications for mantle-melt generation and lithospheric structure. *Journal of the Geological Society* 164, 795–814.

Hoke, L., Hilton, D.R., Lamb, S.H., Hammerschmidt, K., Friedrichsen, H. (1994) ^{3}He evidence for a wide zone of active mantle melting beneath the Central Andes: *Earth and Planetary Science Letters*, 128, 341–355.

Hopp, J., Ionov. D.A. (2011) Tracing partial melting and subduction-related metasomatism in the Kamchatkan mantle wedge using noble gas compositions. *Earth and Planetary Science Letters* 302, 121–131.

Kennedy, B.M., Hiyagon, H., Reynolds, J.H. (1990) Crustal neon: a striking uniformity. *Earth and Planetary Science Letters* 98, 277–286.

Kurz, M.D., Curtice, J., Fornari, D., Geist, D., Moreira, M. (2009) Primitive neon from the center of the Galápagos hotspot. *Earth and Planetary Science Letters* 286, 23–34.

Matsumoto, T., Chen, Y.L., Matsuda, J. (2001) Concomitant occurrence of primordial and recycled noble gases in the Earth's mantle. *Earth and Planetary Science Letters* 185, 35–47.

Moreira, M., Kunz, J., Allègre, C. (1998) Rare gas systematics in popping rock: Isotopic and elemental compositions in the upper mantle. *Science* 279, 1178–1181.

Moreno, H., Clavero, J. (2006) Geología del volcán Villarrica. Regiones de La Araucanía y de Los Lagos. Servicio Nacional de Geología y Minería, Carta Geológica Básica, No. 98, 35 pp., 1 mapa escala 1:50.000.

Newell, D.L., Jessup, M.J., Hilton, D.R., Shaw, C.A., Hughes, C.A. (2015) Mantle-derived helium in hot springs of the Cordillera Blanca, Peru: Implications for mantle-to-crust fluid transfer in a flat-slab subduction setting. *Chemical Geology* 417, 200–209.

Plank, T. (2005) Constraints from Thorium/Lanthanum on sediment recycling at subduction zones and the evolution of the continents. *Journal of Petrology* 46, 921–944.

Plank, T. (2014) 4.17 - The Chemical Composition of Subducting Sediments. In: Holland, H.D., Turekian, K.K. (Eds.) *Treatise on Geochemistry*. Second Edition, Elsevier, Oxford, 607–629.

Rivera, M., Martin, H., Le Pennec, J.L., Thouret, J.C., Gourgaud, A., Gerbe, M.C. (2017) Petro-geochemical constraints on the source and evolution of magmas at El Misti volcano (Peru). *Lithos* 268–271, 240–259.

Rivera, M., Thouret, J.C., Samaniego, P., Le Pennec, J.L. (2014) The 2006–2009 activity of the Ubinas volcano (Peru): Petrology of the 2006 eruptive products and insights into genesis of andesite magmas, magma recharge and plumbing system. *Journal of Volcanology and Geothermal Research* 270, 122–141.

Rizzo, A.L., Di Piazza, A., de Moor, J.M., Alvarado, G.E., Avard, G., Carapezza, M.L., Mora, M.M. (2016) Eruptive activity at Turrialba volcano (Costa Rica): Inferences from $^{3}He/^{4}He$ in fumarole gases and chemistry of the products ejected during 2014 and 2015. *Geochemistry, Geophysics, Geosystems* 17, 4478–4494.

Robidoux, P., Aiuppa, A., Rotolo, S.G., Rizzo, A.L., Hauri, E.H., Frezzotti, M.L. (2017) Volatile contents of mafic-to-intermediate magmas at San Cristóbal volcano in Nicaragua. *Lithos* 272–273, 147–163.

Robidoux, A.L. Rizzo, F. Aguilera, A. Aiuppa, M. Artale, M. Liuzzo, M. Nazzari, F.Z. (2020) Petrological and noble gas features of Lascar and Lastarria volcanoes (Chile): Inferences on plumbing systems and mantle characteristics. *Lithos* 370–371, 105615.

Samaniego, P., Rivera, M., Mariño, J., Guillou, H., Liorzou, C., Zerathe, S., Delgado, R., Valderrama, P., Scao, V. (2016) The eruptive chronology of the Ampato-Sabancaya volcanic complex (Southern Peru). *Journal of Volcanology and Geothermal Research* 323, 110–128.

Sancho, A. (2019) Rol e implicancias de los volátiles magmáticos en las condiciones pre-eruptivas de los centros eruptivos menores Caburgua y Chaillupén, Andes del Sur, Memoria entregada a la Universidad Mayor en cumplimiento de los requisitos para optar al Título de Geóloga. B.Sc. Thesis, Universidad Mayor, Escuela de Geología, Santiago, 137 pp.

Sarda, P., Staudacher, T., Allègre, C.J. (1988) Neon isotopes in submarine basalts. *Earth and Planetary Science Letters* 91, 73–88.

Simmons, S.F., Sawkins, F.J., Schlutter, D.J. (1987) Mantle-derived helium in two Peruvian hydrothermal ore deposits, *Nature* 329, 429–432.

Thouret, J.-C., Rivera, M., Gerbe, M.-C., Finizola, A., Fornari, M., Azur, G., Gonzales, K. (2005) Ubinas: the evolution of the historically most active volcano in southern Peru. *Bulletin of Volcanology* 67, 557–589.

Witter, J.B., Kress, V.C., Delmelle, P., Stix, J. (2004) Volatile degassing, petrology, and magma dynamics of the Villarrica Lava Lake, Southern Chile. *Journal of Volcanology and Geothermal Research* 134, 303–337.